Discharge estimates with stage-fall-discharge rating curves and ICESat-2 altimetry at backwater-affected virtual stations

Jun Liu[1], Liguang Jiang[2], Monica Coppo Frias[1], and Peter Bauer-Gottwein[1]

[1]Technical University of Denmark
[2]Southern University of Science and Technology

November 21, 2022

Abstract

Satellite altimetry has become an important data source for discharge estimation. Stage-fall-discharge (SFQ) rating curves are necessary for discharge estimation at backwater-affected river reaches because of non-uniqueness of stage-discharge (SQ) relationships. We used a hydrodynamic model to simulate stage, water surface fall, and discharge at six backwater-affected reaches and generated SQ/SFQ rating curves everywhere along the river. The simulated SQ rating curves showed that the uncertainties of the estimated discharge were on the order of 150%. The uncertainties were reduced to less than 35% when using SFQ rating curves in rivers with significant falls. We used ICESat-2 laser altimetry, which synchronously measures stage and fall, to estimate discharge with the simulated SFQ rating curves in the Missouri River. The study highlights the importance of backwater effects for discharge estimation, particularly for VS located upstream of major tributary junctions, and showcases the possibilities of ICESat-2 laser altimetry for EO-based discharge estimation.

Supporting Information for

Discharge estimates with ICESat-2 altimetry and simulated stage-fall-discharge rating curves at backwater-affected virtual stations

Jun Liu[1], Liguang Jiang[2], Monica Coppo Frias[1], Peter Bauer-Gottwein[1]

[1]Department of Environmental Engineering, Technical University of Denmark, Kgs. Lyngby, 2800, Denmark

[2]School of Environmental Science and Engineering, Southern University of Science and Technology, Shenzhen, China

Contents of this file

Text S1-S6

Figure S1 – S3

Table S1

Text S1 – S6

Text S1 Derivation of the rating curves

Flow in rivers is governed by the Saint-Venant equations. The conservation form of momentumequation is:

$$\frac{\mathrm{dQ}}{\mathrm{dt}} + \frac{\partial}{\partial x}\left(\frac{\beta Q^2}{A}\right) + gA\frac{\mathrm{dH}}{\mathrm{dx}} - gA(S_0 - S_f) = 0 \# (1)$$

In equation (1), Q is river discharge (m^3/s), t is time (s), x is river chainage (m), β is momentum coefficient (-),A is the cross-sectional area (m^2), H is the flow depth (m), g is the gravitational constant (9.81 m/ s^{-2}), S_0 is river bed slope (-), S_f is the friction slope (-).

If the inertia terms ($\frac{\mathrm{dQ}}{\mathrm{dt}} + \frac{\partial}{\partial x}\left(\frac{\beta Q^2}{A}\right)$) of the momentum equation can be neglected, we obtain the so-called diffusive wave approximation:

$$\mathrm{gA}\frac{\mathrm{dH}}{\mathrm{dx}} - gA\left(S_0 - S_f\right) = 0\#\left(2\right)$$

The water surface elevation (WSE) of a river section can be measured by gauging stations or satellite altimetry. The changes of WSE along river chainage ($\frac{\partial wse}{\partial x}$) is the water surface slope/fall. The relationship between the water surface fall, changes in depth, and riverbed slope is:

$$S_0 - \frac{\mathrm{dH}}{\mathrm{dx}} = -\frac{\partial wse}{\partial x}\#\left(3\right)$$

Manning's equation is an empirical formula for the friction slope:

$$Q = \frac{1}{n} \bullet A \bullet \left(\frac{A}{P}\right)^{\frac{2}{3}} \bullet {S_f}^{\frac{1}{2}}\#\left(4\right)$$

n is Manning's roughness coefficient ($\frac{s}{m^{\frac{1}{3}}}$), P is the wetted perimeter of the flow (m).

Assuming that the river is wide and the cross section is rectangular with constant river width (w), Manning's equation can be written as:

$$Q = \frac{1}{n} \bullet H^{\frac{5}{3}} \bullet w \bullet {S_f}^{\frac{1}{2}}\#\left(5\right)$$

For the river sections without backwater effects, i.e. in uniform flow conditions, river depth variations along the channel are insignificant, and $\frac{\mathrm{dH}}{\mathrm{dx}} = 0$. From equation (2), we obtain the so-called kinematic wave approximation:

$$S_0 - S_f = 0\ \#\left(6\right)$$

River flow depth can be expressed as the difference between water surface elevation and bed elevation. From equations (5) and (6), we have:

$$Q = \frac{1}{n} \bullet \left(WSE - z_0\right)^{\frac{5}{3}} \bullet w \bullet {S_0}^{\frac{1}{2}}\#\left(7\right)$$

Assuming n, w, and S_0 are constant values at a cross section. This equation is exact for wide rectangular rivers. For the general case, we assume a similar relationship with fitting parameters$a$, b, and z_0 between discharge and WSE, which is the stage-discharge rating curve:

$$Q = a \bullet \left(WSE - z_0\right)^b\ \#\left(8\right)$$

For river reaches affected by backwater, depth changes with chainage are significant, and $\frac{\mathrm{dH}}{\mathrm{dx}} \neq 0$. Combing equations (2) and (3), we have:

$$S_f = \frac{\partial H}{\partial x} - S_0 = \frac{\partial wse}{\partial x}\#\left(9\right)$$

From equation (5), we have the following relationship:

$$Q = \frac{1}{n} \bullet (WSE - z_0)^{\frac{5}{3}} \bullet w \bullet \left(\frac{\partial wse}{\partial x}\right)^{\frac{1}{2}} \# (10)$$

This equation is exact for wide rectangular rivers. For the general case, we assume a similar relationship with fitting parameters c,d, z_s, and d between stage, fall, and discharge, which is the stage-fall-discharge rating curve:

$$Q = c \bullet \left(\frac{\partial wse}{\partial x}\right)^{d} \bullet (WSE - z_s)^{e} \ \# (11)$$

Text S2. Hydrodynamic model description

MIKE Hydro River (MIKE hereinafter), a one-dimensional (1D) hydrodynamic model based on shallow-water equations (Vreugdenhil, 1994), is used to simulate stage and fall along the chainage. The required inputs for MIKE are river reaches, cross sections, Manning-Strickler coefficient (Ks), and boundary conditions of discharge. The following texts describe cross section delineation (Text S3), model parameterization (Text S4), and estimation of boundary discharge (Text S5). A summary of model performance is presented in Text S6.

Text S3. Cross section delineation

ICESat-2 ALT03 provides detailed measurements of land surface height with specific passing dates. The river bank and water surface can be monitored from space, which forms the exposed cross section shape (Ma et al., 2020; Neumann et al., 2019; Xu et al., 2021). ICESat-2 measures a larger portion of the river cross section during low-flow seasons, and the submerged portion of the cross section is smaller. We processed ICESat-2 ALT03 products in low-flow seasons, and the processed data are used to delineate exposed parts of the cross sections. ALT03 products are the laser points with noise. Hampel Filter is used for data smoothing (Pearson et al., 2016).

The submerged part of the cross section is assumed to follow the power-law hydraulic geometry relationship (Lawrence, 2007). The power-law relationship needs two parameters, i.e., a depth (distance between the ICESat-2 measured water surface elevation and river bed) and a shape parameter (beta), which can be calibrated (Vatankhah, 2020) by hydraulic inversion. The determination of submerged depth and beta are introduced in the following section. Fig. S3 shows one of the cross sections in Amur River with the exposed part monitored by ICESat-2 ALT03 and the submerged part delineated by the power-law relationship with two candidate parameters.

Text S4. Parameterization

As described above, each cross section should determine a submerged depth and a shape parameter beta. Considering the limited WSE measurements, we assume that the submerged depth is uniform both upstream and downstream of the river confluences and that beta is constant along the entire river channel. Thus, we calibrate two effective submerged depths in each river reach, one for the reach upstream river confluence and one for the reach downstream river confluence, and a shape parameter beta. Additionally, the roughness parameter, i.e., Ks, needs to be determined for the hydrodynamic model. These parameters are determined by hydraulic inversion, which uses optimization methods to search a set of optimum parameters matching, in a least-squares sense, observed and simulated WSE (Frias et al., 2022).

Satellite altimetry measured WSE is only available at satellite passing dates. The outputs of MIKE models are time-continuous, but only the simulations with the same dates of satellite altimetry are used for calibration. To run the model with time-continuous simulations over simulation periods of several years is computationally demanding in an inverse parameter estimation workflow. Therefore, we simplify the calibration problem by assuming that the flow is in a steady state on satellite passing dates, and the model is run only on the dates with satellite altimetry. The simplification significantly increases computational efficiency, and the calibrated parameters can be transferred back to MIKE for unsteady simulations (Kittel et al., 2021; Liu et al., 2021). The objective function for the inversion problem is:

$$\varphi = \sqrt{\frac{1}{N}\sum_{i=1}^{N}\left(\mathrm{WSE}_{sim,\ \ i} - \mathrm{WSE}_{obs,\ i}\right)^2} \# (13)$$

In the equation, $\mathrm{WSE_{sim}}$ is the simulated WSE where ICESat-2 observations exist (at all chainage and time),$\mathrm{WSE_{obs}}$ is the ICESat-2 ALT13, N is the total number of ICESat-2 ALT13 WSE observations. A global optimization package (i.e., the Shuffled Complex Evolution Algorithm) in Statistical Parameter Optimization Tool for Python (SPOTPY) is used for parameter calibration in the present study to avoid interference from improper initial parameter settings and local optima (Houska et al., 2015).

Text S5. Estimation of boundary discharge

River discharge is a necessary boundary condition for hydrodynamic models. However, obtaining high spatio-temporal resolution discharge estimates covering the operating period of ICESat-2 for the studied river reaches (for both mainstream and major tributaries) is challenging. We only found in-situ discharge for one of our cases (the Missouri River and its tributary, the Yellowstone River) from the United States Geological Survey. Therefore, the Global Flood Awareness System (GloFAS) reanalysis product is used as reference discharge for the other river sections, providing daily discharge estimates for global rivers from 1979 to the present (Harrigan et al., 2020). The time series of the daily discharge for mainstream and tributary are shown in Fig.S2.

Text. S6 Performance of hydrodynamic models

Hydrodynamic models are calibrated against the WSE from ICESat-2 ALT13 and ALT08 depending on the width of the river and validated against the WSE measurements from Sentinel-3A/B or Jason-3. The range of model misfit (in terms of RMSE) at the six case study sites is [0.62 m, 1.36 m]. The results are displayed with scatter plots in Fig.2. The calibrated parameters, i.e., upstream low-flow depth, downstream low-flow depth, beta, and Strickler coefficient, inverted by the optimization algorithm are effective values, which compensate for the irregularly varying effects of width, bed elevation, and vegetation in space and time.

The validation results indicated by the root mean square error (RMSE) of the six VS ranges from 0.83 m to 3.14 m, as shown with the curve plots in Fig 2. The simulations mismatch the satellite altimetry at VS-3 (Amazon-Negro River) and VS-6 (Niger-Benue River), with RMSE of 3.14 m and 3.02 m, respectively. For the Niger River section, we found two large dams upstream of the studied river segments (The Kainji Dam and the Jeba Dam, Lehner et al., 2011), and it appears from the GLOFAS hydrographs that those are not modeled in the GloFAS system. Because the measurements of WSE by Sentinel-3B show that the water surface is relatively stable in the low-flow seasons, we hypothesize that the natural river flow has been altered and that the alteration is not reproduced in the GloFAS discharge product. For the Amazon-Negro River, the GloFAS discharge is significantly higher than the in-situ observations in other years (Fig. S3). Thus we have a calibrated upstream depth of 37.88 m to compensate for the high discharge. Similar situations can also be found in the Amur- Zeya River (Zeya Reservoir locates upstream of Zeya), and the Missouri-Yellowstone River (Fort Peck Lake locates upstream of the Missouri River). Inaccurate discharge of the Zeya River may influence the fall of the mainstream. For the Missouri-Yellowstone River, we replaced the GloFAS discharge with in-situ observations for both the mainstream and the tributary.

Figure S1-S3

Figure S1

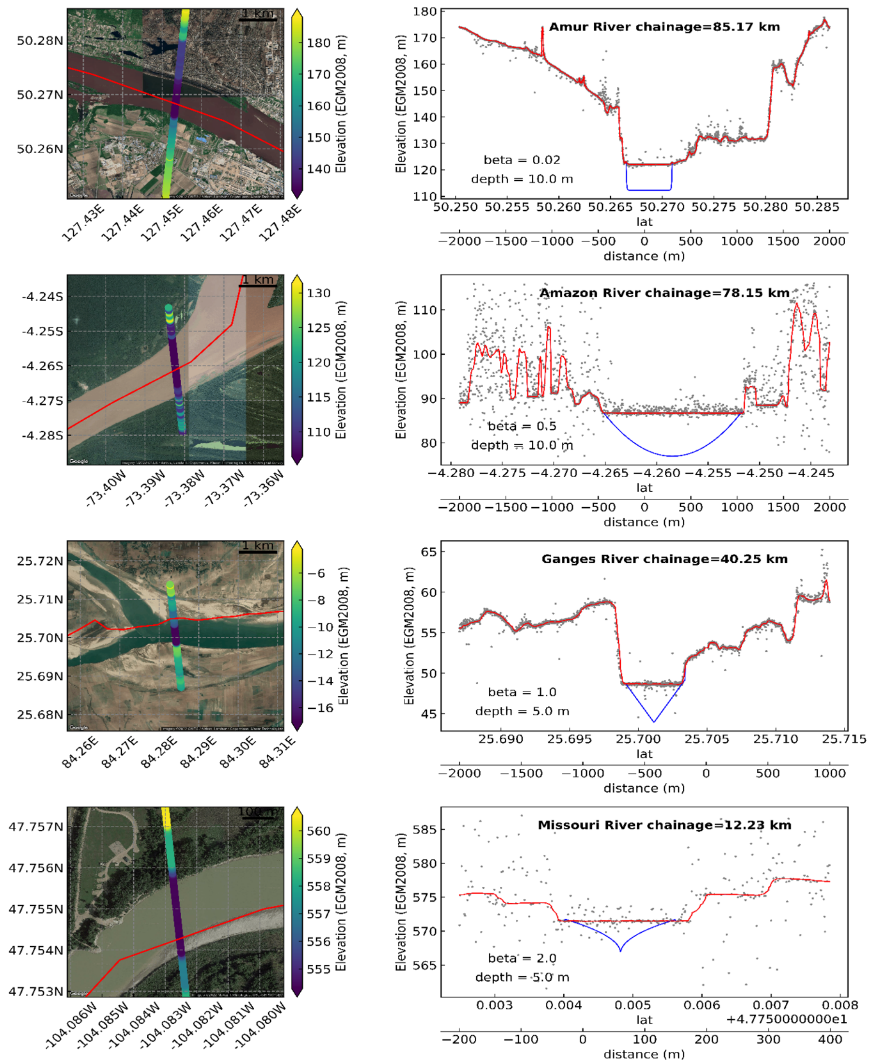

Figure S1. Example of river cross-section geometry. (a) shows the river center line in red and ICESat-2 global geolocated photon (ATL03) measured heights. (b) shows the exposed topography of the river channel measured by ICESat-2 ALT03 in low-flow seasons, shown in gray points. The solid red line is the smoothed values of ICESat-2 ALT03. The submerged topography is delineated under the assumption that the channel cross-section geometry follows the power law relationship described in (Lawrence, 2007), shown in a solid blue line. The parameters that need to be optimized are submerged depth (distance between ICESat-2 measurements and river bed) and beta (shape parameter).

Figure S2

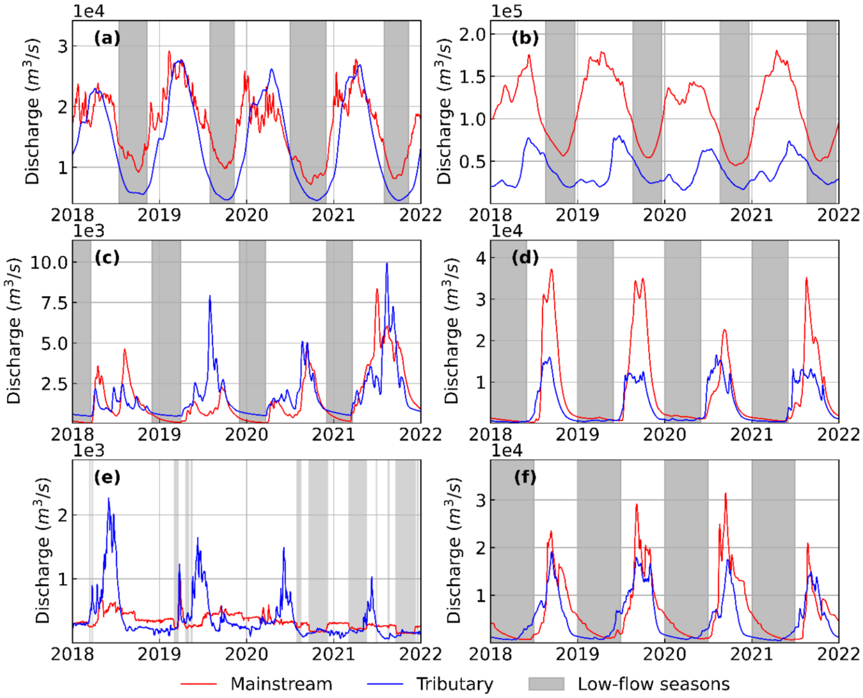

Figure S2. GloFAS daily discharge of mainstream and tributary in (a) Amazon River and Ucayali River, (b) Amazon River and Negro River, (c) Amur River and Zaya River, (d) Ganges River and Ghaghara River (e) Missouri River and Yellowstone River, and (f) Niger River and Benue River. The gray-shadow areas show the low-flow seasons.

Figure S3

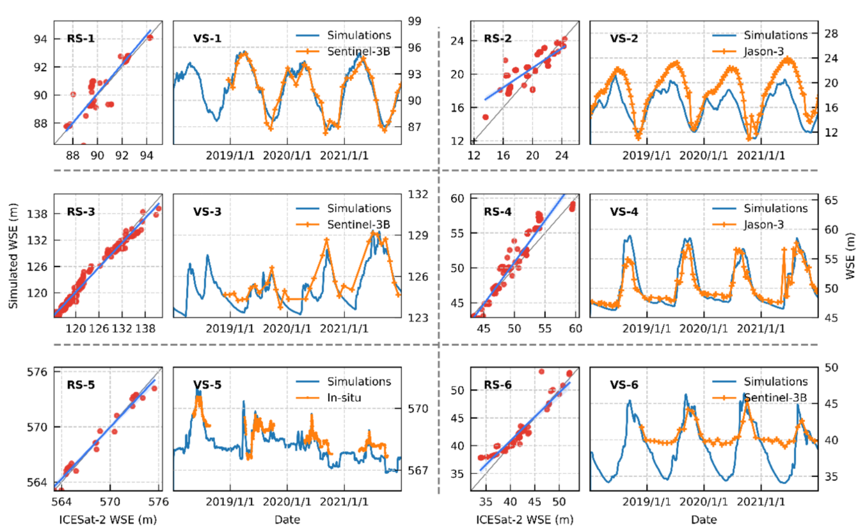

Figure S3. Calibration and validation results of the hydrodynamic models. For each river reach (separated by the gray dash lines), the left column is the calibration results of the steady-state solver along the river section. The right column is the validation results of time-series-continuous water surface elevation between simulations (MIKE hydro River model) and satellite altimetry at Sentinel-3 A/B or Jason-3 virtual stations.

Table S1

Mainstream	Major tributary	River reach length (km)	chainage of river confluences (km)	chainage of gauging/virtual
Amazon	Ucayali	139.076	53.53	32.353
Amazon	Negro	141.22	96.32	73.19
Amur	Zeya	157.165	95.68	76.78
Ganges	Ghaghara	171.74	91.10	68.22
Missouri	Yellowstone	93.82	54.21	43.159
Niger	Benue	173.146	144.19	114.16

Table 1. Information of the study cases, including the name of mainstream rivers and the corresponding tributary rivers, the length of the river reaches for modeling, the validation datasets and location, and the values of the calibrated parameters organized with the order of upstream low-flow depth (m), downstream low-flow depth (m), beta and Strickler roughness coefficient ($m^{1/3}$/s), calibration and validation results.

References

Frias, M.C., Liu, S., Mo, X., Nielsen, K., Ranndal, H., Jiang, L., Ma, J., Bauer-gottwein, P., 2022. River hydraulic modelling with ICEsat-2 land and water surface elevation 1–27.

Harrigan, S., Zsoter, E., Alfieri, L., Prudhomme, C., Salamon, P., Wetterhall, F., Barnard, C., Cloke, H., Pappenberger, F., 2020. GloFAS-ERA5 operational global river discharge reanalysis 1979-present. Earth Syst. Sci. Data 12, 2043–2060. https://doi.org/10.5194/essd-12-2043-2020

Houska, T., Kraft, P., Chamorro-Chavez, A., Breuer, L., 2015. SPOTting model parameters using a ready-made python package. PLoS One 10, e0145180.

Kittel, C.M.M., Hatchard, S., Neal, J.C., Nielsen, K., Bates, P.D., Bauer-Gottwein, P., 2021. Hydraulic model calibration using CryoSat-2 observations in the Zambezi catchment. Water Resour. Res. 1–19. https://doi.org/10.1029/2020wr029261

Lawrence, D.S., 2007. Analytical derivation of at-a-station hydraulic-geometry relations. J. Hydrol. 334, 17–27. https://doi.org/10.1016/j.jhydrol.2006.09.021

Lehner, B., Liermann, C.R., Revenga, C., Vörömsmarty, C., Fekete, B., Crouzet, P., Döll, P., Endejan, M., Frenken, K., Magome, J., Nilsson, C., Robertson, J.C., Rödel, R., Sindorf, N., Wisser, D., 2011. High-resolution mapping of the world's reservoirs and dams for sustainable river-flow management. Front. Ecol. Environ. 9, 494–502. https://doi.org/10.1890/100125

Liu, J., Jiang, L., Bandini, F., Kittel, C.M.M., Balbarini, N., Hansted, N.G., Grosen, H., Bauer-Gottwein, P., 2021. Spatio-temporally Varying Manning Roughness in Rivers and Streams: A calibration approach using in-situ water level and UAS altimetry.

Ma, Y., Xu, N., Liu, Z., Yang, B., Yang, F., Wang, X.H., Li, S., 2020. Satellite-derived bathymetry using the ICESat-2 lidar and Sentinel-2 imagery datasets. Remote Sens. Environ. 250, 112047. https://doi.org/10.1016/j.rse.2020.112047

Neumann, T.A., Martino, A.J., Markus, T., Bae, S., Bock, M.R., Brenner, A.C., Brunt, K.M., Cavanaugh, J., Fernandes, S.T., Hancock, D.W., Harbeck, K., Lee, J., Kurtz, N.T., Luers, P.J., Luthcke, S.B., Magruder, L., Pennington, T.A., Ramos-Izquierdo, L., Rebold, T., Skoog, J., Thomas, T.C., 2019. The Ice, Cloud, and Land Elevation Satellite – 2 mission: A global geolocated photon product derived from the Aadvanced Ttopographic Llaser Aaltimeter Ssystem. Remote Sens. Environ. 233, 111325. https://doi.org/10.1016/j.rse.2019.111325

Paris, A., Dias de Paiva, R., Santos da Silva, J., Medeiros Moreira, D., Calmant, S., Garambois, P., Collischonn, W., Bonnet, M., Seyler, F., 2016. Stage-discharge rating curves based on satellite altimetry and modeled discharge in the Amazon basin. Water Resour. Res. 52, 3787–3814.

Pearson, R.K., Neuvo, Y., Astola, J., Gabbouj, M., 2016. Generalized Hampel Filters. EURASIP J. Adv. Signal Process. 2016. https://doi.org/10.1186/s13634-016-0383-6

Vatankhah, A.R., 2020. Optimum simple and complex power-law channels. SN Appl. Sci. 2, 1–18. https://doi.org/10.1007/s42452-020-03197-w

Vreugdenhil, C.B., 1994. Numerical methods for shallow-water flow. Springer Science & Business Media.

Xu, N., Ma, X., Ma, Y., Zhao, P., Yang, J., Wang, X.H., 2021. Deriving Highly Accurate Shallow Water Bathymetry from Sentinel-2 and ICESat-2 Datasets by a Multitemporal Stacking Method. IEEE J. Sel. Top. Appl. Earth Obs. Remote Sens. 14, 6677–6685. https://doi.org/10.1109/JSTARS.2021.3090792

Discharge estimates with stage-fall-discharge rating curves and ICESat-2 altimetry at backwater-affected virtual stations

Jun Liu[1], Liguang Jiang[2], Monica Coppo Frias[1], and Peter Bauer-Gottwein[1]

[1]Department of Environmental Engineering, Technical University of Denmark, Kgs. Lyngby, 2800, Denmark.

[2]School of Environmental Science and Engineering, Southern University of Science and Technology, Shenzhen, China.

Corresponding author: Jun Liu (juli@dtu.dk)

Key Points:

- We quantified the uncertainties of stage-discharge (SQ) rating curves for discharge estimates at backwater-affected virtual stations
- Stage-fall-discharge (SFQ) rating curves reduce the uncertainties of discharge estimates at backwater-affected virtual stations
- ICESat-2 measures water level simultaneously along six tracks enabling the calculation of falls, and thus SFQ can be used for discharge estimates

Abstract

Satellite altimetry has become an important data source for discharge estimation from space. Stage-fall-discharge (SFQ) rating curves are necessary for accurate discharge estimation at backwater-affected river reaches because of the non-uniqueness of stage-discharge (SQ) relationships in such cases. We used a hydrodynamic model to simulate stage, fall (water surface slope), and discharge at six backwater-affected reaches and generated SQ/SFQ rating curves everywhere along the reaches. For six backwater-affected virtual stations (VS), the simulated SQ rating curves showed that the relative uncertainties of the estimated discharge were on the order of 150%. In contrast, the uncertainties were reduced to less than 35% when using SFQ rating curves in rivers with significant falls. Subsequently, we used ICESat-2 laser altimetry, which synchronously measures stage and fall, to estimate discharge with the simulated SFQ rating curves in the Missouri River. The study highlights the importance of backwater effects for discharge estimation, particularly for VS located upstream of major tributary junctions, and showcases the possibilities of ICESat-2 laser altimetry for EO-based discharge estimation.

Plain Language Summary

A significant portion of global VS, where satellite altimetry provides precise river stage measurements, is affected by backwater from downstream tributary confluences. In this situation, a SFQ rating curve is recommended instead of the SQ rating curve to estimate discharge. However, it is generally impossible to estimate instantaneous water surface fall from traditional nadir altimetry missions, e.g., Jason-1/2/3, Sentinel-3A/B. ICESat-2 laser altimetry measures the stage using three pairs of laser beams with an across-track distance of around 3.3 km. Consequently, the water surface fall can be estimated, providing an opportunity to use SFQ from space. In the present study, we showcase the influence of backwater on SQ relationships and the necessity to use SFQ rating curves for accurate discharge estimates in backwater-affected reaches. We then illustrate the potential of using ICESat-2 measured stage and water surface fall with SFQ rating curves to estimate discharge at backwater-affected VS in the Missouri River. Our study showcases the possibilities of quantifying the impacts of variable backwater conditions on SQ rating curves and the options of using ICESat-2 to inform SFQ rating curves and estimate discharge.

1 Introduction

River discharge is a fundamental quantity that is required to improve our understanding of the hydrological cycle and inform flood, drought, and water resources management (Gerten, Rost, von Bloh, & Lucht, 2008; Rajsekhar & Gorelick, 2017; Rao et al., 2020). However, on top of data sharing problems, the number of global river gauging stations for discharge records is decreasing, leading to increasing demands for satellite-based discharge retrieval. Virtual stations (VS), located at the intersection between satellite ground track and water bodies, can be established and significantly improve the density of existing hydrometric monitoring networks. Many studies, therefore, developed methods to estimate discharge at VS, such as generating rating curves (Getirana & Peters-Lidard, 2013; Paris et al., 2016; Tourian, Schwatke, & Sneeuw, 2017; E. A. Zakharova, Kouraev, Cazenave, & Seyler, 2006), informing hydrological-hydrodynamic models (Durand et al., 2016; Jiang, Madsen, & Bauer-Gottwein, 2019; Siddique-E-Akbor, Hossain, Lee, & Shum, 2011; Tarpanelli, Barbetta, Brocca, & Moramarco, 2013), and inverting hydraulic models (Sichangi et al., 2016; E. Zakharova, Nielsen, Kamenev, & Kouraev, 2020).

Using stage-discharge (SQ) rating curves to convert stage to discharge is valuable and suitable for operational applications, due to low input data requirements and straightforward modeling concepts. SQ rating curves are commonly used worldwide at in-situ gauging stations. However, rating curves are only valid if section/channel controls govern SQ relationships with constant energy slope (World Meteorological Organization, 2010). When the energy slope varies over time, e.g., due to variable backwater, relationships between stage and discharge become more complex, and the stage does not uniquely determine the discharge. Utilizing SQ rating curves to interpolate discharge series for variable backwater-affected river sections can cause large uncertainties. For instance, Meade et al. (1991) found that backwater from major tributaries downstream caused a varying stage spanning 2-3 m in the Amazon River at a given discharge; Hidayat et al.(2011) used SQ rating curves to estimate discharge in River Mahakam, and the estimated discharge spans more than 2000 m^3/s for a specific stage (the maximum discharge is 3250 m^3/s).

A stage-fall-discharge (SFQ) rating curve should be established to account for variable backwater effects. The fall in the relationship refers to the energy slope, which is approximately equal to the water surface gradient/slope. The fall can be determined by the stage records from the base gauge and an auxiliary reference gauge at some distance from the base gauge, which is known as the twin-gauge approach, documented in standard hydrometric literature (Herschy, 2008; Kennedy, 1984; Mander, 1978; Rantz, 1982). However, it is challenging to find twin VS for backwater-affected river reaches using the existing radar altimetry missions (e.g., Jason-1/2/3, Sentinel-3 A/B) due to the narrow swath widths and wide spacing of ground tracks, and because overpasses at neighboring VS occur at different times. Nevertheless, some studies attempted to densify the spatio-temporal resolution of WSE measurements using multiple satellite missions (Nielsen, Zakharova, Tarpanelli, & Andersen, 2022; Tourian et al., 2016), and interpolation is mandatory for the fall estimates. Paris et al. (2016) estimated a monthly average fall by the interpolated WSE series for one specific VS located at the mouth of the Negro River, and they got an encouraging result showing that the SFQ rating curve outperforms the SQ rating curve for discharge estimates (Nash–Sutcliffe Efficiency improved by 130 - 208%). However, the fall estimates derived from nadir altimetry are uncertain due to the nonsynchronous measurements. Estimating reliable falls for a broad range of river reaches remains challenging.

National Aeronautics and Space Administration (NASA)'s current Ice, Cloud, and land Elevation Satellite-2 (ICESat-2) mission provides new opportunities to inform SFQ rating curves from space. The laser pulses from the ICESat-2 altimeter illuminate three left/right pairs of spots on the surface that, as ICESat-2 orbits Earth, trace out six ground tracks at the time. Left/right spots within each pair are approximately 90 m apart, and pair tracks are approximately 3 km apart in the across-track direction (Rebold, Global, & Photon, 2021). Under normal conditions, each spot can provide WSE at the cross-over point with the river. Thus, the fall can be calculated from the simultaneously monitored WSE along an approximately 6km-long river chainage interval.

The objectives of this study are to (1) investigate the relationship between stage, fall, and discharge at backwater-affected VS using hydrodynamic modeling; (2) quantify the uncertainties of SQ/SFQ rating curves for discharge estimates at specific stages; and (3) showcase the possibilities of using the measurements of water surface elevation and fall from ICESat-2 to estimate discharge with simulated SFQ rating curves.

2 Rating curves at backwater affected virtual stations

VS are the intersections between satellite altimetry ground tracks (e.g., TOPEX/Poseidon, Jason-1/2/3, ENVISAT, and Sentinel-3 A/B) and inland water bodies, from where the altimeters deliver measurements of WSE. Figure 1a shows the VS configuration for Sentinel-3A/B and ICESat-2. The former mission has a ground footprint of approximately 300 m in the along-rack direction, while the latter has a much smaller footprint (~ 17 m). ICESat-2 emits six laser beams and thus synchronously measures WSE at six individual chainage points. Compared with Sentinel-3 A/B, ICESat-2 laser altimetry enables more detailed surveys of the water surface and the surrounding topography. The WSE obtained from the six laser beams can be used to determine water surface fall, which is an essential hydraulic variable.

The relationship between WSE and discharge at the VS in Figure 1a is complicated because of the backwater from the large tributary. Figure 1b shows an idealized example of the river longitudinal profile. The influence of backwater gradually vanishes from the confluence to the most upstream point. However, the chainage interval affected by backwater varies in length depending on the river channel bed slope, mainstream and tributary discharge, river width, channel resistance, etc. Typically, backwater effects are significant in an interval of a few tens of kilometers upstream of major tributaries. Figure 1c shows the relationship between stage and discharge of the mainstream and the tributary. Evidently, different combinations of mainstream discharge and tributary discharge can create a close or equal stage at the VS. While the discharge is distinguishable when we use the water surface fall as an ancillary reference for a specific stage (see the contour plots in Figure 1d). Thus, we can combine the stage-discharge table (Figure 1c) and the fall-discharge table (Figure 1d) to determine the discharge uniquely at backwater-affected VS. Furthermore, the SFQ rating curve can be built and used by merging the two tables under such situations.

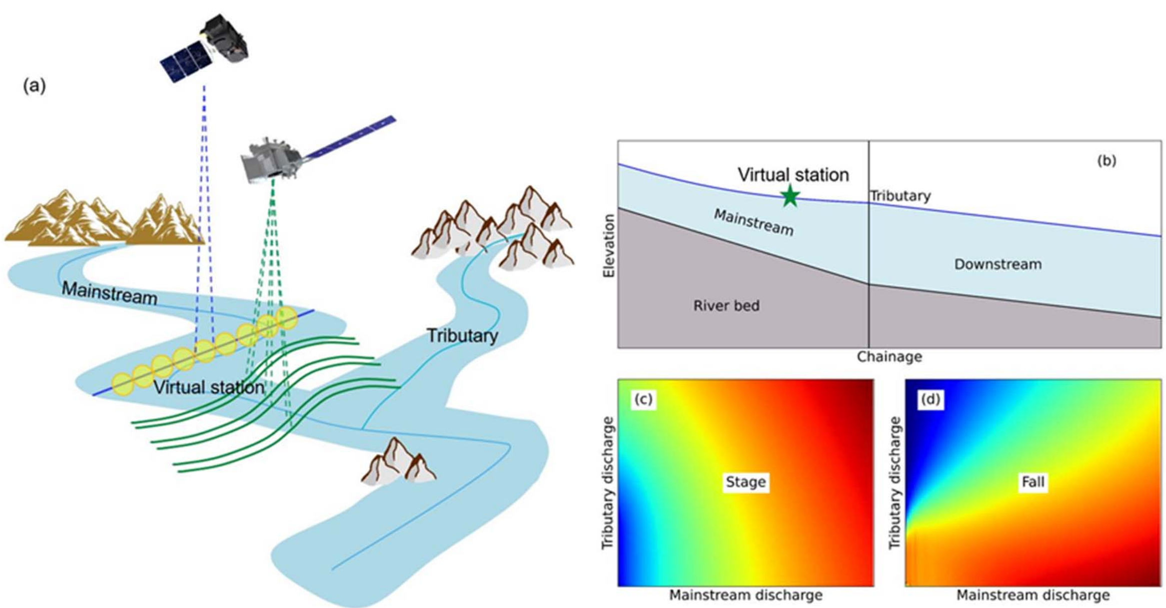

Figure 1. Schematic diagram. (a) VS of Sentinel-3 A/B and ICESat-2 at a river section just upstream of a major tributary confluence; (b) longitudinal profile of the mainstream with the

location of the large tributary shown as a vertical black line and the location of VS; (c) Contour plot of the relationship between mainstream discharge, tributary discharge, and the stage at the virtual station; (d) Contour plot of the relationship between mainstream discharge, tributary discharge, and the water surface fall at the virtual station

SQ/SFQ rating curves are based on the kinematic and diffusive wave approximations of the Saint-Venant equations, respectively (WMO, 2010a). In the present study, we use the following equations to represent SQ rating curves (equation 1) and the SFQ rating curves (equation 2). The derivation of the formulas can be found in Text S1.

$$Q = a \cdot (WSE - z_0)^b \tag{1}$$

$$Q = c \cdot \left(\frac{\partial WSE}{\partial x}\right)^d \cdot (WSE - z_s)^e \tag{2}$$

In the equations, Q is the estimated discharge, WSE is the water surface elevation measured by satellite altimetry, and $\frac{\partial WSE}{\partial x}$ is the water surface fall. a, b, z_0, c, d, e, and z_s are parameters that will be fitted using least squares optimization with simulated/observed pairs of the stage, fall, and discharge at a specific river section.

3 Case studies

3.1 study sites

We hand-picked six prototypical backwater-affected VS on large rivers worldwide to show the impact of backwater on SQ relationships and the necessity of using SFQ rating curves in such situations. The selected river reaches have the following characteristics:

(1) High-quality discharge estimates are available for the mainstream and the major tributaries.
(2) The river reaches have significant seasonality of discharge.
(3) The VS are potentially affected by backwater effects from major downstream tributary confluences.

The selected river reaches are the Amazon River around the confluence of Amazon River and Ucayali River (VS-1), the Amazon River around the confluence of Amazon River and Negro River (VS-2), Amur River around the confluence of Amur River and Zeya River (VS-3), Missouri River around the confluence of Missouri River and Yellowstone River (VS-4), Ganges River around the confluence of Ganges River and Ghaghara River (VS-5), and Niger River around the confluence of Niger River and Benue River (VS-6). See maps of the study sites in Figure 2. Statistical information on the studied river reaches can be found in Table S1.

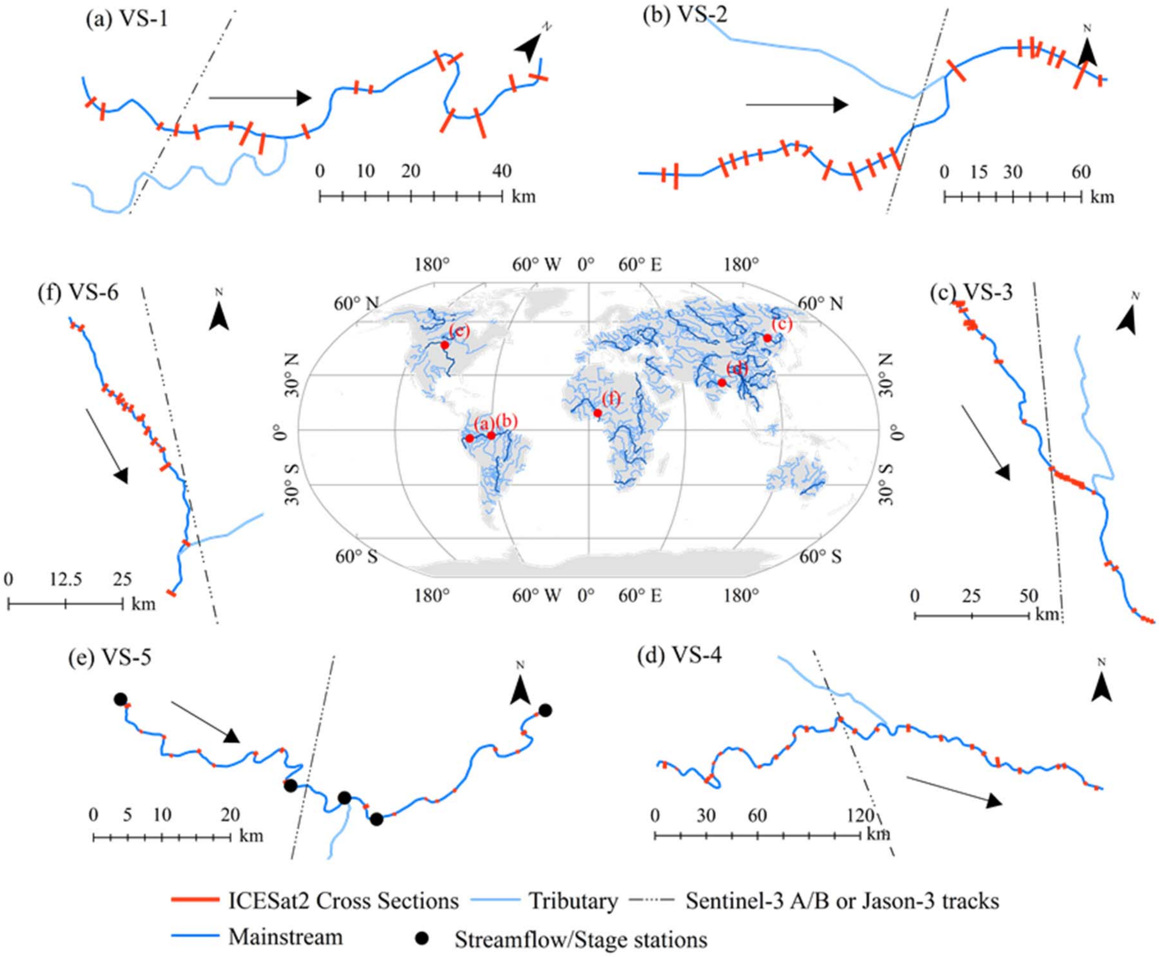

Figure 2. Locations of the study sites. The ground map in the center is the annual average discharge derived from GloFAS. Subplots (a – f) are the partially enlarged view of the study cases, including (a) the Amazon-Ucayali River, (b) the Amazon-Negro River, (c) the Amur River, (d) the Ganges River, (e) the Missouri River, (f) the Niger River. In each river section, mainstream, tributary, the ground track of Sentinel-3/Jason-3, and river cross sections are shown. The black arrow line indicates the flow direction of the mainstream.

3.2 Satellite altimetry

ICESat-2, equipped with the Advanced Topographic Laser Altimeter System (ATLAS), was launched in September 2018. Raw photon data collected by the altimeter has been processed to different levels and product types. The level-2 products (ALT03) are based on the photon flight times and are bias-corrected by temperature and voltage effects (Rebold et al., 2021). The along-track resolution of ALT03 is approximately 70 cm, which enables detailed measurements of land surface topography.

ALT08 and ALT13 are level-3A post-processed datasets. ALT08 provides estimates of terrain height and canopy height and cover with a resampled along-track resolution of 100 m

(Neuenschwander et al., 2021). ALT13 offers measurements for inland water bodies, such as WSE, along-track slope, and roughness. Land and narrow inland water bodies have been masked and excluded from the ATL13 product (Jasinski et al., 2021). Compared with ALT03 and ALT08 for water surface monitoring, ALT13 is convenient because data volumes are relatively small. The evaluation results of ALT13 over water bodies by previous studies showed a high accuracy of WSE. For example, the average water level estimation error is 0.12 m of the lower Mississippi River (Xiang, Li, Zhao, Cai, & Li, 2021) and 0.27 m of the upper Yangtze River (Guo, Jin, & Zhang, 2022). However, narrow rivers typically have fewer records of WSE in ALT13 products. ALT08 is used as an appropriate substitute.

Ancillary satellite altimetry datasets, including Sentinel-3 A/B and Jason-3, are used to locate the VS and independently validate the hydrodynamic model simulations. Global descriptions and assessments of these radar altimetry missions over large river systems indicate a promising performance in WSE measurements (Biancamaria et al., 2018; Huang et al., 2019; Jiang, Nielsen, Dinardo, Andersen, & Bauer-Gottwein, 2020; Kittel, Jiang, Tøttrup, & Bauer-Gottwein, 2021).

3.3 Hydrodynamic model

A one-dimensional hydrodynamic model is used to simulate the SQ/SFQ rating curves everywhere along the river chainage, including the locations of VS. The required inputs for the model are river reaches, cross sections, and boundary conditions of discharge. Vector river reaches are extracted from the global river networks with a length of about 150 km for each case (Yan et al., 2019).

Satellite altimetry and hydraulic relationship are incorporated to delineate the cross sections because in-situ measurements of cross sections for the abovementioned river reaches are unobserved or inaccessible. Specifically, ICESat-2 ALT03 topographic data are used to measure the exposed part of the cross sections, including water surface and river banks. The spatial resolution of ALT03 photon measurements of heights is around 0.7 m, much higher than most publicly accessible digital elevation models (DEM). The finer resolution appropriately captures the height changes in water-land interaction areas. When the satellite passing dates are in low-flow seasons, a larger portion of the river cross section can be measured by ICESat-2 laser photons. The submerged part of the cross section cannot be observed by satellite EO but can be parameterized with the power-law geometry relationship (Lawrence, 2007; Vatankhah, 2020). The parameters can be estimated by hydraulic inversion. A detailed description and an example of the method for cross section delineation can be seen in the supporting materials (Figure S1).

Boundary conditions of discharge are critical for hydrodynamic modeling. However, in-situ gauging stations in the studied cases are sparse, and many mainstream and tributary discharge data are inaccessible. Moreover, fewer discharge records cover the period of ICESat-2 observations (after 2018), and only the Missouri River and Yellowstone River have sufficient discharge data. Thus, daily discharge from Global Flood Awareness System (GloFAS) reanalysis is used as boundary condition for the other cases (Harrigan et al., 2020). The Modified Kling–Gupta efficiency skill score (KGESS) of GloFAS against in-situ observations is generally higher than 0.6 (optimum value is 1) in Amazon, Amur, Amur, and Ganges River basins (see Figure 5 in Harrigan et al. (2020)). The supporting materials provide detailed technical descriptions of hydrodynamic model configurations, parameterization, and validation.

4 Results

4.1 Simulated rating curves at VS

The calibration error of the hydrodynamic models is in the range of [0.62 m, 1.36 m]. The optimum parameters are then transferred to the fully dynamic HD models to simulate WSE and fall with continuous time series input. The validation error is within [0.83m, 3.14 m] for the six VS (from Jason-1/2/3 and Sentinel-3 A/B), which indicates the outputs from the model are reasonable for further analyses (See Supporting information S1).

The simulated SQ pairs show distinct non-uniqueness at the six selected VS, which cannot be described using a uniform rating curve, as shown in the left column of Figure 3 for each case. Once a particular stage with an assumed error of 0.1 m is used to estimate discharge, the uncertainty may range from 51% (VS-2) to 144% (VS-5). It should be noted that uncertainties of discharge listed in the subplots are not the maximum values, as we selected the certain stage occasionally (the black boxes in the subplots of Figure 3). The uncertainties could be higher for other stages even with the same error. The scattered SQ relationships are attributed to variable backwater because the river cross-sections and the resistance were stable during the simulation. The influences of backwater depend on river channel topography, the discharge of tributary and mainstream, and the distance between the VS and the confluence. Thus, the non-unique patterns of the SQ relationship vary among VS. For example, the scattered pattern of the SQ relationship at VS-1 is significant because the river channel is flatter. Likewise, the SQ relationship is distinctly scattered at VS-5, partly due to the tributary discharge being much larger than the mainstream discharge, resulting in more powerful backwater effects. The influences of backwater at VS-6 are relatively weak because the VS locates 30 km upstream river confluence, and the river channel is relatively steep with a larger river slope.

In contrast, SFQ relationships are more robust in determining discharge, as shown in the right columns of Figure 3 for each VS. We can clearly find the impact of backwater on fall (from a few to tens of cms per km) from the subplots. The assumption of SQ is not valid anymore. But discharge is distinguishable from a fall in the same stage. Once a specific stage is used for discharge estimates, the discharge value can be further determined by the reference to fall, and the uncertainties of the estimated discharge are much smaller. Therefore, the SFQ rating curve is an appropriate solution to dealing with backwater effects and providing accurate discharge estimates.

However, the accuracy of discharge estimates with SFQ rating curves depends on the precision of measured stage and fall. Assuming that ICESat-2-measured WSE and fall have uncertainties of 10 cm and 2 cm/km, respectively, the estimated discharge still has large uncertainties in flat rivers with small slopes, such as the Amazon River and Ganges River. The accuracy of the estimated discharge is higher in rivers with large surface gradients, such as the Amur, Missouri, and Niger rivers (Figure 3).

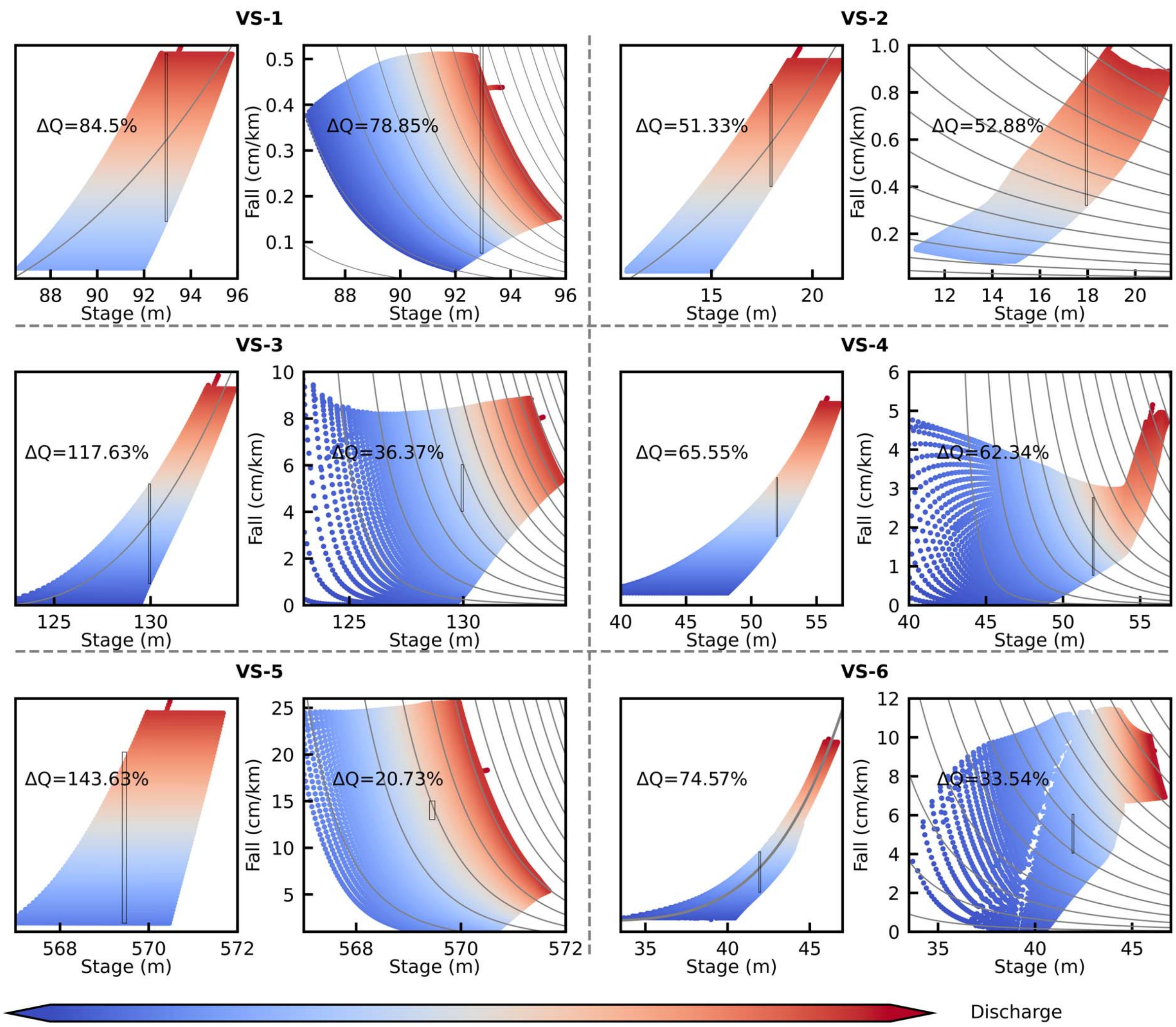

Figure 3. The simulated stage, fall, and discharge pairs at virtual stations (VS). For each study case (divided by gray dash lines), the left column is the simulated stage-discharge pairs shown with a scattered colormap, and the black box indicates a specific stage (with an uncertainty of 0.1 m) corresponds to a range of discharge ($[Q_{max}, Q_{min}]$), while $\Delta Q = (Q_{max} - Q_{min})/Q_{estimate} \times 100$; the right column shows the simulated stage, fall (y-axis), and discharge pairs in a scattered colormap. The black boxes show a couple of stages (with an uncertainty of 0.1 m), and fall (the uncertainty is 2 cm/km) corresponds to a range of discharge. All the subplots share the same color bar, representing the discharge changes. Specifically, deep blue represents low discharge, and deep red represents high discharge.

4.2 Discharge estimates in real case

Missouri River around the confluence of Missouri River and Yellowstone River, where in-situ observations of stage and discharge for the mainstream and the tributary are accessible, is selected to validate the applicability of the simulated SFQ rating curves and to illustrate the possibility of using ICESat-2 measurements of water surface stage and fall to estimate discharge.

In this case, satellite altimetry and in-situ observations of WSE are used for hydrodynamic model parameter calibration to get the rating curves with higher accuracy.

Figure 4 shows that the backwater effects are significant in the high flow periods according to the stage measured by satellite altimetry and the twin gauges. The water surface fall monitored by ICESat-2 increases from 3.24 cm/km on 2019-06-19 to 10.23 cm/km on 2019-07-28 and to 18.42 cm/km on 2021-09-13. The largest water surface fall, 24.69 cm/km, occurred on 2020-03-17. ICESat-2 measurements have high accuracy compared with in-situ observations.

Discharge is estimated using ICESat-2 measured stage and fall with the simulated SQ/SFQ rating curves, respectively, and the results are shown in Figures 4c and 4d. The RMSE of the estimated discharge is 89.85 m^3/s using SQ rating curves, and the value is 4.55 m^3/s when using the SFQ rating curves. SFQ rating curves significantly improved the accuracy of discharge estimates on these backwater-affected dates. Taking the day 2019-06-19 as an example, the mainstream discharge was 260.52 m^3/s, and the discharge from the tributary was 1432.83 m^3/s. The water surface fall is significantly reduced, which can also be seen from the stages observed by the twin-gauges and ICESat-2 altimetry (Figure 4b). In this case, the backwater effects from downstream were significant. SQ rating curves overestimated the discharge because of the higher WSE raised by backwater. In contrast, the SFQ rating curve estimated the discharge correctly. Clearly, the effects diminish as the ratio of tributary discharge to mainstream discharge decreases. On 2021-09-13, mainstream discharge (271.28 m3/s) was higher than the tributary discharge (86.08 m^3/s), and the water surface fall was high on that day, indicating the backwater effects are weak. Therefore, the differences in the estimated discharge using SQ and SFQ rating curves were small. As shown in Figure 4b, the water surface condition in the backwater-affected area was mutually influenced by discharge from mainstream and tributary, and thus, the accuracy of discharge estimates varies significantly using SQ rating curves but not SFQ. Therefore, use of water surface fall as a reference is essential for accurate discharge estimates.

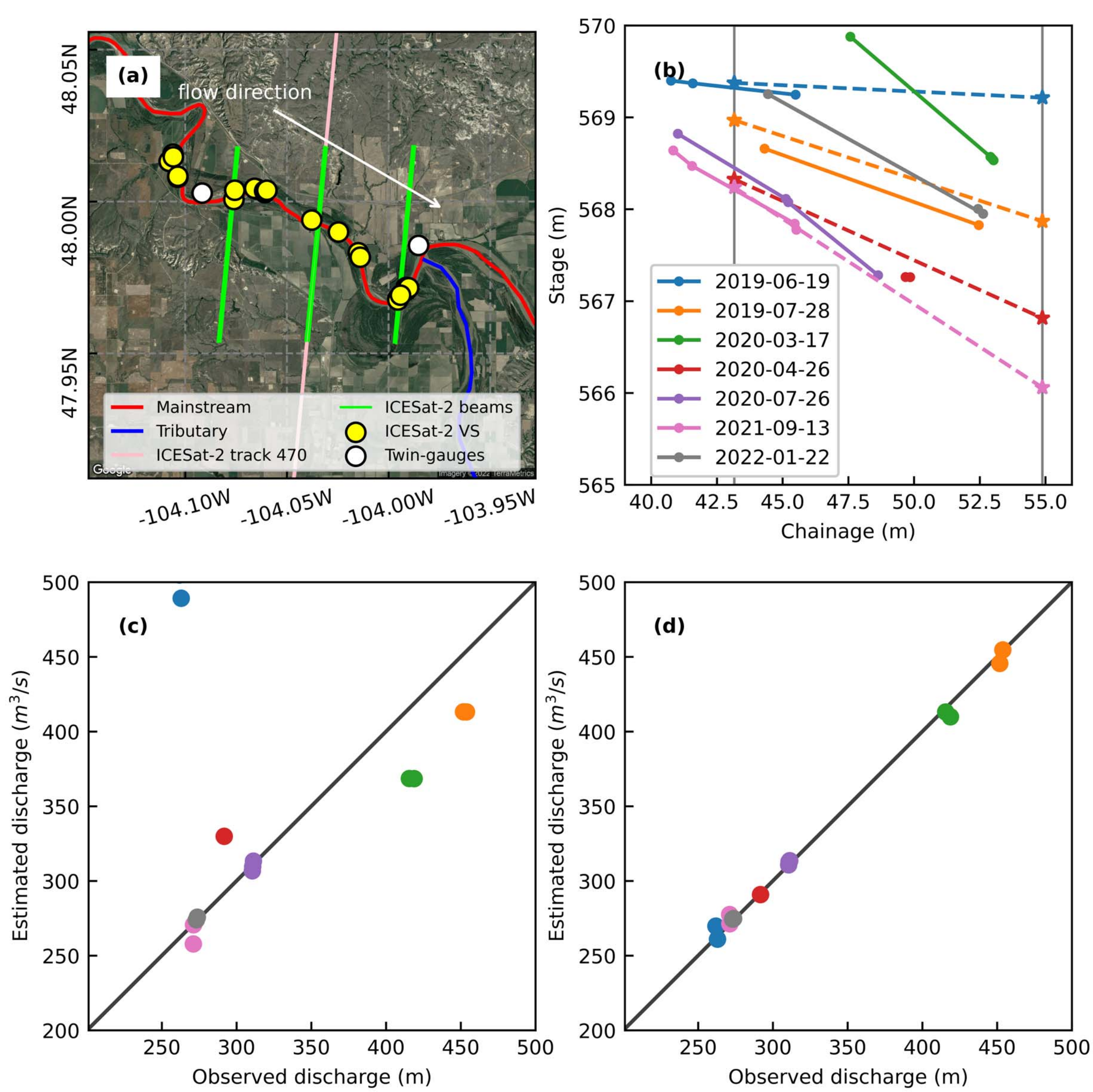

Figure 4. (a) Map of Missouri River and Yellowstone River river channels with the locations of twin gauges, ICESat-2 reference tracks, laser beams, and the drifting virtual stations. (b) shows the water surface fall estimated by ICESat-2 (solid lines) and twin gauges (dash lines). Please be aware that the in-situ observations of the stage are missing for a few months at the two gauging sites; (c) and (d) are the discharge estimated by stage-discharge(SQ) rating curves and stage-fall-discharge (SFQ) rating curves with water surface stage and fall from ICESat-2 measurements.

5 Discussion and Conclusions

Satellite altimetry measures the dynamic changes in water surface heights that are closely related to river flow. Discharge estimated from space is valuable for studying fluvial systems under changing climates considering the status quo of sparse gauging networks. Remotely sensed WSE coupled with hydraulic relationships, e.g., SQ rating curves, have been proven to be applicable for discharge estimation (Durand et al., 2021; Getirana & Peters-Lidard, 2013; Kouraev, Zakharova, Samain, Mognard, & Cazenave, 2004; Paris et al., 2016; Tarpanelli et al., 2013). Simple SQ relationships are suitable for stable and simple river channels, but the relationships are non-unique at backwater affected VS. Our study revealed that the scattered SQ relationship at backwater-affected VS may cause an error of up to ~143.63% for discharge estimates at a specific stage. With such large uncertainties, the estimated discharge is untrustworthy. We thus conclude that Jason-1/2/3, Sentinel-3 A/B, or other nadir altimeters that only measure WSE are incapable of estimating discharge with SQ rating curves in backwater affected VS. One promising solution for this problem is the use of SFQ rating curves (Mansanarez et al., 2016; Petersen-Øverleir and Reitan, 2009; WMO, 2010). The uncertainties of the estimated discharge decreased significantly when using SFQ rating curves. With the same uncertainty of stage (0.1 m), the errors of estimated discharge reduced from 143.63% with SQ rating curves to 20.73% using SFQ rating curves, assuming an uncertainty of water surface fall of 2.0 cm/km at VS-5.

To use SFQ rating curves for discharge estimates from space, we are facing the challenge of getting water surface fall in sync with WSE measurements. The only current satellite mission providing accurate fall estimates is ICESat-2, thanks to the simultaneous measurements with six laser beams. The possibilities of using ICESat-2 altimetry with SFQ rating curves to estimate discharge have been illustrated by this study for the first time (Figure 4). However, the shortcomings of ICESat-2 are apparent and must be emphasized here. The mission has a long repeat period of 91 days. The measurements of the water surface are drifting, which is different from other satellite missions with fixed ground tracks and monitoring sites over rivers. Moreover, inland water surfaces are often covered by clouds, thus not every Icesat-2 track provides valid water surface elevation data. ICESat-2 has measurement errors of the stage of about 10 centimeters over rivers (Guo et al., 2022; Lao, Wang, Nie, Xi, & Wang, 2022). These measurement errors propagate to the estimated water surface fall. The across-track distance of ICESat-2 measurements is around 6 km, and the uncertainty of fall is thus a few centimeters per kilometer, depending on the actual distance along chainage between ICESat-2 tracks and the number of ICESat-2 points used in slope estimation. Thus, the accuracy of discharge estimates is low in flat rivers, such as the Amazon River (Figure 3). These shortcomings result in sparse time series of the estimated discharge with significant uncertainty at specific river sections. Prospectively, the gaps can be bridged by the upcoming satellite missions such as the Surface Water and Ocean Topography (SWOT) mission, Unmanned Ariel System altimetry (Bandini et al., 2017, 2020), and advanced altimetry processing techniques such as fully-focused synthetic aperture radar (Egido & Smith, 2017), which can provide synchronous and accurate measurements of stage and fall.

Simple hydrodynamic models were used to generate rating curves because of the lack of measurements from both in-situ gauges and satellites. Although there are considerable differences between modelled and observed WSE, the models are deemed appropriate for illustrating the effect of backwater on rating curves (Figure 3). Moreover, the models can be used to estimate the length of the river section upstream of the tributary junction that is affected by backwater, thus determining whether a VS is affected by backwater or not. Finally, the models are useful for uncertainty analysis of rating curves and error propagation from stage/fall to discharge. ICESat-2 measured stage and fall, in combination with SFQ rating curves and can be used to get more accurate discharge estimates, which have promising prospects for application.

The upcoming Surface Water and Ocean Topography (SWOT) mission will provide WSE and slope at high spatio-temporal resolution. SWOT uses Ka-band interferometric synthetic aperture radar (InSAR) to map surface water elevation, slope, and water mask on a 21-day repeat orbit with high accuracy (Biancamaria, Lettenmaier, & Pavelsky, 2016; Durand et al., 2021). The state-of-art SWOT-oriented discharge estimating algorithms have shown great potential for discharge estimates, which have been validated in many large rivers (Brisset, Monnier, Garambois, & Roux, 2018; Garambois & Monnier, 2015; Gleason & Smith, 2014). However, many SWOT-oriented methods are based on Manning's equation, assuming that river depth changes along river chainage are insignificant (Yoon et al., 2016). Such algorithms will fail to provide accurate discharge estimates in backwater-affected reaches. Combining stage and slope measurements from SWOT, and SFQ rating curves for estimating discharge at backwater affected river reaches offers a promising alternative.

Acknowledgments

This study was supported by the ChinaWaterSense project (File number: 8087-00002B), the National Key Research and Development Program of China project (2018TFE0106500), and the European Space Agency in the scope of the Hydrocoastal project. The first author expresses thanks to China Scholarship Council for supporting his study.

Data Availability Statement Data

The data sets used in this study are all publicly available. ICESat-2 ALT03, ALT08, and ALT13 were downloaded from https://nsidc.org/data/icesat-2, Sentinel-3 A/B, and Jason-3 altimetry were downloaded from Hydroweb (https://hydroweb.theia-land.fr/). MIKE HYDRO River hydrodynamic model was provided by DHI (https://www.mikepoweredbydhi.com). The shapefiles of river reach were extracted from a dataset of global river networks downloaded from https://figshare.com/articles/dataset/A_data_set_of_global_river_networks_and_corresponding_water_resources_zones_divisions/8044184. The spacecraft image of Sentinel-3 A/B was downloaded from https://commons.wikimedia.org/wiki/File:Sentinel-3_spacecraft_model.svg. The spacecraft image of ICESat-2 was downloaded from https://icesat-2.gsfc.nasa.gov/observatory-graphics.

References

Bandini, F., Butts, M., Jacobsen, T. V., & Bauer-Gottwein, P. (2017). Water level observations from unmanned aerial vehicles for improving estimates of surface water–groundwater interaction. *Hydrological Processes*, *31*(24), 4371–4383. https://doi.org/10.1002/hyp.11366

Bandini, F., Sunding, T. P., Linde, J., Smith, O., Jensen, I. K., Köppl, C. J., … Bauer-Gottwein, P. (2020). Unmanned Aerial System (UAS) observations of water surface elevation in a small stream: Comparison of radar altimetry, LIDAR and photogrammetry techniques. *Remote Sensing of Environment*. https://doi.org/10.1016/j.rse.2019.111487

Biancamaria, S., Lettenmaier, D. P., & Pavelsky, T. M. (2016). The SWOT Mission and Its Capabilities for Land Hydrology. In *Surveys in Geophysics* (Vol. 37). https://doi.org/10.1007/s10712-015-9346-y

Biancamaria, S., Schaedele, T., Blumstein, D., Frappart, F., Boy, F., Desjonquères, J. D., …

Niño, F. (2018). Validation of Jason-3 tracking modes over French rivers. *Remote Sensing of Environment*, *209*(June 2017), 77–89. https://doi.org/10.1016/j.rse.2018.02.037

Brisset, P., Monnier, J., Garambois, P. A., & Roux, H. (2018). On the assimilation of altimetric data in 1D Saint–Venant river flow models. *Advances in Water Resources*, *119*(March 2017), 41–59. https://doi.org/10.1016/j.advwatres.2018.06.004

Corbett, D. M. (1943). *Stream-gaging procedure*. US Department of the Interior.

Durand, M., Gleason, C. J., Garambois, P.-A., Bjerklie, D., Smith, L. C., Roux, H., … Monnier, J. (2016). An intercomparison of remote sensing river discharge estimation algorithms from measurements of river height, width, and slope. *Water Resources Research*, *52*(6), 4527–4549.

Durand, M., Gleason, C. J., Pavelsky, T. M., Frasson, R. P. de M., Turmon, M. J., David, C. H., … et al. (2021). A framework for estimating global river discharge from the Surface Water and Ocean Topography satellite mission. *Earth and Space Science Open Archive*, 43. https://doi.org/10.1002/essoar.10508946.1

Egido, A., & Smith, W. H. F. (2017). Fully Focused SAR Altimetry: Theory and Applications. *IEEE Transactions on Geoscience and Remote Sensing*, *55*(1), 392–406. https://doi.org/10.1109/TGRS.2016.2607122

Garambois, P. A., & Monnier, J. (2015). Inference of effective river properties from remotely sensed observations of water surface. *Advances in Water Resources*, *79*, 103–120. https://doi.org/10.1016/j.advwatres.2015.02.007

Gerten, D., Rost, S., von Bloh, W., & Lucht, W. (2008). Causes of change in 20th century global river discharge. *Geophysical Research Letters*, *35*(20), 1–5. https://doi.org/10.1029/2008GL035258

Getirana, A. C. V., & Peters-Lidard, C. (2013). Estimating water discharge from large radar altimetry datasets. *Hydrology and Earth System Sciences*, *17*(3), 923–933. https://doi.org/10.5194/hess-17-923-2013

Gleason, C. J., & Smith, L. C. (2014). Toward global mapping of river discharge using satellite images and at-many-stations hydraulic geometry. *Proceedings of the National Academy of Sciences of the United States of America*, *111*(13), 4788–4791. https://doi.org/10.1073/pnas.1317606111

Guo, X., Jin, S., & Zhang, Z. (2022). *Evaluation of Water Level Estimation in the Upper Yangtze River from ICESat-2 Data*. *2*, 2260–2264. https://doi.org/10.1109/piers53385.2021.9695146

Harrigan, S., Zsoter, E., Alfieri, L., Prudhomme, C., Salamon, P., Wetterhall, F., … Pappenberger, F. (2020). GloFAS-ERA5 operational global river discharge reanalysis 1979-present. *Earth System Science Data*, *12*(3), 2043–2060. https://doi.org/10.5194/essd-12-2043-2020

Herschy, R. W. (2008). *Streamflow measurement*. CRC press.

Hidayat, H., Vermeulen, B., Sassi, M. G., F. Torfs, P. J. J., & Hoitink, A. J. F. (2011). Discharge estimation in a backwater affected meandering river. *Hydrology and Earth System Sciences*, *15*(8), 2717–2728. https://doi.org/10.5194/hess-15-2717-2011

Huang, Q., Li, X. D., Han, P. F., Long, D., Zhao, F. Y., & Hou, A. Z. (2019). Validation and application of water levels derived from Sentinel-3A for the Brahmaputra River. *Science China Technological Sciences*, *62*(10), 1760–1772. https://doi.org/10.1007/s11431-019-9535-3

Jasinski, M. F., Stoll, J. D., Hancock, D., Robbins, J., Nattala, J., Morison, J., … C. (2021). *ATLAS/ICESat-2 L3A Along Track Inland Surface Water Data, Version 5* (D. NASA National Snow & I. D. C. D. A. A. Center, Eds.). https://doi.org/10.5067/ATLAS/ATL13.005.

Jiang, L., Madsen, H., & Bauer-Gottwein, P. (2019). Simultaneous calibration of multiple hydrodynamic model parameters using satellite altimetry observations of water surface elevation in the Songhua River. *Remote Sensing of Environment*, *225*, 229–247. https://doi.org/10.1016/J.RSE.2019.03.014

Jiang, L., Nielsen, K., Dinardo, S., Andersen, O. B., & Bauer-Gottwein, P. (2020). Evaluation of Sentinel-3 SRAL SAR altimetry over Chinese rivers. *Remote Sensing of Environment*, *237*(October 2019), 111546. https://doi.org/https://doi.org/10.1016/j.rse.2019.111546

Kennedy, E. J. (1984). *Discharge ratings at gaging stations*. Department of the Interior, US Geological Survey.

Kittel, C. M. M., Jiang, L., Tøttrup, C., & Bauer-Gottwein, P. (2021). Sentinel-3 radar altimetry for river monitoring - A catchment-scale evaluation of satellite water surface elevation from Sentinel-3A and Sentinel-3B. *Hydrology and Earth System Sciences*, *25*(1), 333–357. https://doi.org/10.5194/hess-25-333-2021

Kouraev, A. V., Zakharova, E. A., Samain, O., Mognard, N. M., & Cazenave, A. (2004). Ob' river discharge from TOPEX/Poseidon satellite altimetry (1992-2002). *Remote Sensing of Environment*, *93*(1–2), 238–245. https://doi.org/10.1016/j.rse.2004.07.007

Lao, J., Wang, C., Nie, S., Xi, X., & Wang, J. (2022). Monitoring and Analysis of Water Level Changes in Mekong River from ICESat-2 Spaceborne Laser Altimetry. *Water*, *14*(10), 1613.

Lawrence, D. S. (2007). Analytical derivation of at-a-station hydraulic-geometry relations. *Journal of Hydrology*, *334*(1–2), 17–27. https://doi.org/10.1016/j.jhydrol.2006.09.021

Mander, R. J. (1978). *Aspects of unsteady flow and variable backwater*. Wiley: Chichester.

Mansanarez, V., Le Coz, J., Renard, B., Lang, M., Pierrefeu, G., & Vauchel, P. (2016). Bayesian analysis of stage-fall-discharge rating curves and their uncertainties. *Water Resources Research*, *52*(9), 7424–7443.

Meade, R. H., Rayol, J. M., Da Conceicão, S. C., & Natividade, J. R. G. (1991). Backwater effects in the Amazon River basin of Brazil. *Environmental Geology and Water Sciences*, *18*(2), 105–114. https://doi.org/10.1007/BF01704664

Neuenschwander, A. L., Pitts, K. L., Jelley, B. P., Robbins, J., Klotz, B., Popescu, S. C., … Sheridan, R. (2021). *ATLAS/ICESat-2 L3A Land and Vegetation Height, Version 5*. https://doi.org/10.5067/ATLAS/ATL08.005.

Nielsen, K., Zakharova, E., Tarpanelli, A., & Andersen, O. B. (2022). River levels from multi mission altimetry , a statistical approach. *Remote Sensing of Environment*, *270*(December

2021). https://doi.org/10.1016/j.rse.2021.112876

Paris, A., Dias de Paiva, R., Santos da Silva, J., Medeiros Moreira, D., Calmant, S., Garambois, P., … Seyler, F. (2016). Stage-discharge rating curves based on satellite altimetry and modeled discharge in the Amazon basin. *Water Resources Research*, *52*(5), 3787–3814.

Petersen-Øverleir, A., & Reitan, T. (2009). Bayesian analysis of stage-fall-discharge models for gauging stations affected by variable backwater. *Hydrological Processes*, *23*(21), 3057–3074. https://doi.org/10.1002/hyp.7417

Rajsekhar, D., & Gorelick, S. M. (2017). Increasing drought in Jordan: Climate change and cascading Syrian land-use impacts on reducing transboundary flow. *Science Advances*, *3*(8), 1–16. https://doi.org/10.1126/sciadv.1700581

Rantz, S. E. (1982). *Measurement and computation of streamflow* (Vol. 2175). US Department of the Interior, Geological Survey.

Rao, M. P., Cook, E. R., Cook, B. I., D'Arrigo, R. D., Palmer, J. G., Lall, U., … Webster, P. J. (2020). Seven centuries of reconstructed Brahmaputra River discharge demonstrate underestimated high discharge and flood hazard frequency. *Nature Communications*, *11*(1), 1–10. https://doi.org/10.1038/s41467-020-19795-6

Rebold, T., Global, A. I.-L. A., & Photon, G. (2021). *ATLAS / ICESat-2 L2A Global Geolocated Photon Data , Version 5*.

Sichangi, A. W., Wang, L., Yang, K., Chen, D., Wang, Z., Li, X., … Kuria, D. (2016). Estimating continental river basin discharges using multiple remote sensing data sets. *Remote Sensing of Environment*, *179*, 36–53. https://doi.org/10.1016/j.rse.2016.03.019

Siddique-E-Akbor, A. H. M., Hossain, F., Lee, H., & Shum, C. K. (2011). Inter-comparison study of water level estimates derived from hydrodynamic-hydrologic model and satellite altimetry for a complex deltaic environment. *Remote Sensing of Environment*, *115*(6), 1522–1531. https://doi.org/10.1016/j.rse.2011.02.011

Tarpanelli, A., Barbetta, S., Brocca, L., & Moramarco, T. (2013). River discharge estimation by using altimetry data and simplified flood routing modeling. *Remote Sensing*, *5*(9), 4145–4162. https://doi.org/10.3390/rs5094145

Tourian, M. J., Schwatke, C., & Sneeuw, N. (2017). River discharge estimation at daily resolution from satellite altimetry over an entire river basin. *Journal of Hydrology*, *546*, 230–247. https://doi.org/10.1016/j.jhydrol.2017.01.009

Tourian, M. J., Tarpanelli, A., Elmi, O., Qin, T., Brocca, L., Moramarco, T., & Sneeuw, N. (2016). Spatiotemporal densification of river water level time series by multimission satellite altimetry. *Water Resources Research*, *52*(2), 1140–1159.

Vatankhah, A. R. (2020). Optimum simple and complex power-law channels. *SN Applied Sciences*, *2*(8), 1–18. https://doi.org/10.1007/s42452-020-03197-w

WMO. (2010a). *Manual on Stream Gauging Volume II -Computing of Discharge*.

WMO. (2010b). *Manual on stream gauguing*.

Xiang, J., Li, H., Zhao, J., Cai, X., & Li, P. (2021). Inland water level measurement from spaceborne laser altimetry: Validation and comparison of three missions over the Great

Lakes and lower Mississippi River. *Journal of Hydrology*, *597*(68), 126312. https://doi.org/10.1016/j.jhydrol.2021.126312

Yan, D., Wang, K., Qin, T., Weng, B., Wang, H., Bi, W., … Abiyu, A. (2019). A data set of global river networks and corresponding water resources zones divisions. *Scientific Data*, *6*(1), 1–11. https://doi.org/10.1038/s41597-019-0243-y

Yoon, Y., Garambois, P., Paiva, R. C. D., Durand, M., Roux, H., & Beighley, E. (2016). Improved error estimates of a discharge algorithm for remotely sensed river measurements: Test cases on Sacramento and G aronne Rivers. *Water Resources Research*, *52*(1), 278–294. Retrieved from https://doi.org/10.1002/2015WR017319

Zakharova, E. A., Kouraev, A. V., Cazenave, A., & Seyler, F. (2006). Amazon River discharge estimated from TOPEX/Poseidon altimetry. *Comptes Rendus - Geoscience*, *338*(3), 188–196. https://doi.org/10.1016/j.crte.2005.10.003

Zakharova, E., Nielsen, K., Kamenev, G., & Kouraev, A. (2020). River discharge estimation from radar altimetry: Assessment of satellite performance, river scales and methods. *Journal of Hydrology*, *583*(June 2019), 124561. https://doi.org/10.1016/j.jhydrol.2020.124561